AD-A206 546

OFFICE OF NAVAL RESEARCH

GRANT N00014-89-J-1178

R&T Code 413q001-01

Technical Report No. 22

IN-SITU STRESS MEASUREMENTS DURING
THERMAL OXIDATION OF SILICON

by

E. Kobeda* and E. A. Irene

Prepared for Publication

in the

The Journal of Vacuum Science Technology

University of North Carolina
Department of Chemistry
Chapel Hill, NC

*current address: The Microelectronics Center
of North Carolina
Research Triangle Park, NC 27709

89 3 30 088

REPORT DOCUMENTATION PAGE

1a. REPORT SECURITY CLASSIFICATION	1b. RESTRICTIVE MARKINGS
Unclassified	

2a. SECURITY CLASSIFICATION AUTHORITY	3. DISTRIBUTION/AVAILABILITY OF REPORT
	Approved for public release; distribution unlimited.
2b. DECLASSIFICATION/DOWNGRADING SCHEDULE	

4. PERFORMING ORGANIZATION REPORT NUMBER(S)	5. MONITORING ORGANIZATION REPORT NUMBER(S)
Technical Report #22	

6a. NAME OF PERFORMING ORGANIZATION	6b. OFFICE SYMBOL (If applicable)	7a. NAME OF MONITORING ORGANIZATION
UNC Chemistry Dept.		Office of Naval Research (Code 413)

6c. ADDRESS (City, State and ZIP Code)	7b. ADDRESS (City, State and ZIP Code)
CB# 3290, Venable Hall University of North Carolina Chapel Hill, NC 27599-3290	Chemistry Program 800 N. Quincy Street Arlington, Virginia 22217

8a. NAME OF FUNDING/SPONSORING ORGANIZATION	8b. OFFICE SYMBOL (If applicable)	9. PROCUREMENT INSTRUMENT IDENTIFICATION NUMBER
Office of Naval Research		Grant #N00014-89-J-1178

8c. ADDRESS (City, State and ZIP Code)	10. SOURCE OF FUNDING NOS.			
Chemistry Program 800 N. Quincy Street, Arlington, VA 22217	PROGRAM ELEMENT NO.	PROJECT NO.	TASK NO.	WORK UNIT NO.

11. TITLE (Include Security Classification) IN-SITU STRESS MEASUREMENTS DURING THERMAL OXIDATION OF SILICON

12. PERSONAL AUTHOR(S)
E.A. Irene

13a. TYPE OF REPORT	13b. TIME COVERED	14. DATE OF REPORT (Yr., Mo., Day)	15. PAGE COUNT
Interim Technical	FROM _____ TO _____	March 14, 1989	20

16. SUPPLEMENTARY NOTATION

The Journal of Vacuum Science Technology

17. COSATI CODES			18. SUBJECT TERMS (Continue on reverse if necessary and identify by block number)
FIELD	GROUP	SUB. GR.	

19. ABSTRACT (Continue on reverse if necessary and identify by block number)

A two beam laser reflection technique was used to measure SiO_2 film stress during Si oxidation, i.e. in-situ at the growth temperature. Results show a higher compressive intrinsic film stress near the $Si-SiO_2$ interface and a lower stress in the bulk of the SiO_2 film. Thermal stress is also measured by monitoring the SiO_2 film covered Si substrate curvature changes during temperature excursions. Our new results are in general agreement with previous ex-situ stress measurements and may indicate that film stress, being highest at the interface, influences the interface reaction in Si oxidation.

20. DISTRIBUTION/AVAILABILITY OF ABSTRACT	21. ABSTRACT SECURITY CLASSIFICATION
UNCLASSIFIED/UNLIMITED ☒ SAME AS RPT. ☐ DTIC USERS ☐	Unclassified

22a. NAME OF RESPONSIBLE INDIVIDUAL	22b. TELEPHONE NUMBER (Include Area Code)	22c. OFFICE SYMBOL
Dr. David L. Nelson	(202) 696-4410	

DD FORM 1473, 83 APR   EDITION OF 1 JAN 73 IS OBSOLETE.

In-Situ Stress Measurements During

Thermal Oxidation of Silicon

E. Kobeda* and E.A. Irene

Department of Chemistry CB# 3290

The Univ. of North Carolina

Chapel Hill, N.C 27599-3290

*current address: The Microelectronics Center
                  of North Carolina

                  Research Triangle Park, NC 27709

Abstract

A two beam laser reflection technique was used to measure SiO_2 film stress during Si oxidation, i.e. in-situ at the growth temperature. Results show a higher compressive intrinsic film stress near the $Si-SiO_2$ interface and a lower stress in the bulk of the SiO_2 film. Thermal stress is also measured by monitoring the SiO_2 film covered Si substrate curvature changes during temperature excursions. Our new results are in general agreement with previous ex-situ stress measurements and may indicate that film stress, being highest at the interface, influences the interface reaction in Si oxidation.

Introduction

The advent of smaller and faster MOS devices has facilitated the need for thinner gate oxides (<200A) and lower process temperatures (<900°C). These requirements constrain Si oxidation kinetics to a region which is not well described by the currently accepted linear-parabolic oxidation model (1). In particular, this model does not explain the anomalously high oxidation rates observed in the early stages of oxidation (1-4).

A number of studies have reported the observation of film stress as a result of Si oxidation (5-8). An intrinsic stress, σ_i, originates from the molar volume change when converting Si to SiO_2, and a thermal expansion stress, σ_{th}, arises from the thermal contraction mismatch which results upon cooldown from oxidation. The intrinsic stress increases with decreasing oxidation temperature, and thus will be even more important for future device fabrication at lower temperatures. Usually the total residual stress, $\sigma_i + \sigma_{th}$, is measured at room temperature. However, as will be shown below, the in-situ stress measurement under oxidation conditions enables the uncoupling of the total stress into the two components. There are differing views on how stress may affect oxidation. Some models consider how stress alters the interface reaction (9-12) while others focus on effects on the stress altered transport of oxidant through the oxide (13-15).

We report new experimental results on film stress measured both at the oxidation temperature during film growth and upon cooling to room temperature. These results show initially high intrinsic film stress which undergoes relaxation as oxidation proceeds. Our results are discussed in terms of a contribution to the interface reaction at the $Si-SiO_2$ interface, since the stress is highest at this position and available data indicates that this process is more important than diffusion in the very early stages of Si oxidation (16). We also report the measurement of thermal stress during thermal cycling, and obtain experimental values for the elastic constants of SiO_2.

Experimental Procedures

All film stress measurements were carried out using commercially available p-type, 2 Ω-cm, (100) Si wafers which were 5 cm in diameter and 75 µm thick, but which were cleaved to form ~3x4 cm samples. Prior to cleaving, the original wafers received a pre-oxidation at 1000°C to prevent any contamination from Si dust as a result of scribing. After removal of this protective oxide in concentrated HF, the samples were cleaned using a modified RCA method (17) prior to final experimental oxidations.

Stress measurements at the oxidation temperature were performed using a modification of the laser reflection technique previously reported (8). The modified apparatus is depicted in Figure 1. The essential elements include a plate type beamsplitter (BS1) which splits light from a He-Ne laser (6328Å)

into two orthogonal beams which are made parallel by aligning the mirrors (M1 and M2) and the reflecting prism. The beams are transmitted through a second beamsplitter (BS2) and reflected into an oxidation furnace using the mirrror M3. After reflecting from the sample, the beams return to M3 and are reflected to a larger flat mirror M4 by the beamsplitter BS2 to increase the reflection path length and hence the measurement sensitivity. The beams are then returned to a measurement screen to determine the separation distance which can be used to calculate the wafer curvature (8). If oxidation results in warpage of the Si wafer, then a deviation in the initial separation of the beams is observed. Calibration procedures were previously described (8).

The oxidation furnace, which was placed in the path of the parallel light beams in the stress measurement apparatus, consisted of a resistively heated fused silica tube. A constant flow of gaseous N_2 taken from a liquid N_2 source was maintained inside the furnace except during oxidation where ultra high purity O_2 (less than 1 ppm H_2O and 0.5 ppm hydrocarbons) was used. All furnace components were constructed of fused silica. All temperatures are reported with a variation of ~ 3°C, which is attributed to the small size of the hot zone. The water content inside the furnace was monitored constantly in the effluent gas using a capacitance hygrometer. Figure 1 also includes an H_2O fused silica bubbler which was connected in series with the gas feed line to clean the furnace between runs, and which is followed by extensive drying in N_2 before experimental runs. The furnace

endcap had an optically flat strain-annealed pyrex window to allow
entrance and exit of the laser beams without deviation or
significant absorption loss.

To allow for easier sample alignment, a fused SiO_2 wedge was
used to allow alteration of the reflection plane height. The
sample carrier which was also constructed of fused SiO_2, contained
a slotted protrusion cut at a slight angle from the normal. The
sample wafer edge rested loosely in this slot.

For intrinsic stress measurements at the oxidation
temperature, samples were pre-oxidized at 1100°C to ~ 4000 A in a
manner similar to that reported by EerNisse (6) so as to provide a
thick backside oxide, and the front side oxide was removed using
an oxide etch procedure previously reported (8). Since under the
oxidation conditions used in this study, the rate of oxidation for
a thick film on the back side of the wafer is negligible compared
to the bare front side, and the film is in a relatively stress-
free state when grown at high temperatures, curvature changes
during oxidation can be directly attributed to film growth on the
front surface. These samples were also cleaned as usual except
that the HF dip was omitted.

The furnace was kept at room temperature in flowing N_2 during
alignment to minimize oxide growth resulting from back diffusion
of O_2 and H_2O from the laboratory ambient into the furnace while
the end cap was off. After alignment of the sample, the furnace
was ramped to the oxidation temperature and allowed to stabilize,
in order to measure the initial curvature point. Then the ambient

was switched to O_2 and the curvature was monitored with time. Since the film thickness could not be measured directly during oxidation with this system, it was estimated using the "optimized X_1" technique of Massoud (4). Thickness calculations were verified on the in-situ measured samples using ellipsometry after the oxidation was complete. Comparison of these measurements to the estimated thicknesses resulted in an average error of ~ 10% in thickness which translates to about 10% error in stress.

The thermal expansion stress was obtained in-situ by measuring the wafer curvature during thermal treatment in the presence of a N_2 ambient. With no oxidation taking place, the change in curvature with temperature is directly related to the thermal expansion stress component. While every effort was made to maintain the dryness of the oxidation ambient, the necessary alignment and sample adjustment procedures, as well as the use of a thick backside oxide that was exposed to the lasboratory ambient, yielded higher than the usual < 5 ppm H_2O levels during the oxidations and simultaneous stress measurements. That the higher H_2O levels (reported below) affect the stress measurements cannot be excluded in the present study and this is discussed further below.

Experimental Results and Discussion
Stress Measurements.

The in-situ experiments allow for the measurement of intrinsic stress separate from the thermal stress. The curvature

changes in the samples which occur during oxidation are monitored

at the oxidation temperature where $\Delta T = 0$ and hence $\sigma_{th} = 0$, as seen

in the equation for σ_{th}:

$$\sigma_{th} = (E/(1-\nu)_f) \Delta\alpha \Delta T \tag{1}$$

where $E/(1-\nu)$ is the composite elastic constant for the film (18)

and $\Delta\alpha$ the difference in the coefficients of thermal expansion

(CTE) between the film (18) and substrate (19). The thermal

stress develops as the sample cools down from the oxidation

temperature, ΔT, resulting in compression in the oxide since the

CTE for Si is greater than SiO_2. When total stress is measured at

room temperature, the intrinsic stress is obtained by subtracting

the thermal stress from the total film stress using the

relationship:

$$\sigma_f = \sigma_i + \sigma_{th} \tag{2}$$

where σ_f is the total film stress and σ_{th} is calculated. The

value for σ_f is obtained using a revised form of Stoney's original

equation (20):

$$\sigma_f = EL_s^2/6(1-\nu)L_f R \tag{3}$$

where $E/(1-\nu)$ is the composite elastic constant for Si (21), L_s

and L_f the substrate and film thickness, respectively, and R the

radius of curvature. Note that this equation is similar to the

general Hookes law formula:

$$\sigma = E \epsilon \tag{4}$$

where Young's modulus E is replaced by the composite elastic

constant $E/(1-\nu)$, and the strain ϵ is represented by $L_s^2/L_f R$.

Figure 2 shows a comparison of in-situ measurements made during

oxidation in the present study to those obtained sample by sample,
i.e. ex-situ, at room temperature (22). The in-situ data is the
average of three runs with an average error of ~ $0.6x10^9$
dynes/cm^2. With about the same error for the previous data, the
in-situ and ex-situ experiments yield the same compressive σ_i
results. Note that all the data show a greater change in
intrinsic stress with thickness in the early stages of oxidation.

The systematic difference in the magnitude of these curves
can possibly be attributed to the fact that the in-situ oxidations
contained about 15 ppm H_2O, while the ex-situ were done in a
conventional double walled furnace having less than 5 ppm H_2O.
H_2O is known to cause relaxation effects (11,23). In addition the
thick backside SiO_2 film may contain adsorbed H_2O which is
released during oxidation and may effect the total curvature.
Also, there may be a question as to whether the thick backside
SiO_2 film changes at all during the measurements under oxidation
conditions.

Figure 3 shows the measured thermal stress as a function of
oxidation temperature, where the slope yields the product $E/(1-\nu)$
$\Delta\alpha$ as shown earlier. A least squares fit to the data in Figure 3
resulted in a slope whose value was less than 10% different from
the literature values of E and ν(18,19) used to calculate $E/(1-\nu)$. This result is favorable when one considers that the
literature values vary by at least this amount. Slight curvature
is seen in the data and is possibly the result of the presence of
~25 ppm of H_2O inside the furnace during the experiment, which

may result in a small amount of oxide growth at the higher

temperatures. This growth will effectively reduce the curvature

change. It should be noted that when the larger ΔT values are

deleted from this data set to account for possible oxidation, a

slope ~15% higher than the original determination is obtained, and

the value for $E/(1-\nu)\Delta\alpha$ is ~ 5% different from the literature

values we use (18,19).

Oxidation Kinetics and Viscous Relaxation Effects

First we consider the shape of the intrinsic stress profile

as shown in Fig. 2. It is observed that σ_i is larger nearer the

Si-SiO$_2$ interface where SiO$_2$ is produced via the interface

reaction between Si and oxidant. The origin of σ_i has been

attributed to the partial confinement of the molar volume change

accompanying the transformation (5,7,9). Based on the fact that

the maximum σ_i found from extrapolation to zero SiO$_2$ thickness is

substantially less that the theoretical value of more than 10^{11}

dynes/cm^2 (7), an initially fast stress relaxation was suggested

for the SiO$_2$ as it is formed which is followed by a much slower

relaxation that is characteristic of the bulk SiO$_2$ viscosity (22).

Several workers (22,23,26) have suggested the existence of a time

dependent viscosity where as the oxide grows the viscosity

increases from an initial low value for the as forming oxide which

is not yet relaxed into the high viscosity form characteristic of

the nearly relaxed network structure. Further relaxation occurs

for the already formed SiO$_2$ as this oxide continuosly exposed to

the oxidation temperature and pushed out from the interface by
newly forming SiO_2, hence yielding the profile in Fig. 2. The time
dependent viscosity was used to explain the production of Si
interstitials (26) and stress relaxation phenomena (22,23) which
occur as the oxidation or annealing times increase. Corroboration
for the stress profile in Fig. 2 was reported (28,29) from
infrared spectroscopy, IR, measurements of SiO_2 films where the
Si--O--Si bond angle and distribution of angles was obtained.
Essentially, it was reported that near the Si-SiO_2 interface, the
angle between adjacent tetrahedra became gradually smaller
indicating a greater packing of SiO_4 tetrahedra near the Si-SiO_2
interface and with about the same thickness scale as in Fig. 2 for
the 800°C oxidation.

Second, from Fig. 2 we consider the extent of the higher
stress regime. It is observed both in the present in-situ
measurements and previous ex-situ measurements (22), that the
extent of the higher σ_i regime is several hundred A. This is
similar to the extent of the initially rapid oxidation regime, L_i,
which is observed for the thermal oxidation of Si and which was
found not to conform to the kinetics predicted from the linear
parabolic model for Si oxidation (1-4). L_i values ranging from 40
to 230 A have been reported from several authors (1,3,24,25). The
qualitative conformity of the rapid oxidation regime with the high
stress regime supports the recently proposed stress enhanced
oxidation model (10,12) that was proposed as an attempt to explain
the effects of σ_i on the interface reaction during thermal

oxidation. This model assumes a proportionality between the linear oxidation rate constant, k_1, as obtained from the linear parabolic model for oxidation, and stress divided by viscosity as:

$$k_1 \propto \sigma_1 / \eta \qquad (5)$$

where η is the oxide viscosity. This model is derived from the notion that the relaxation of the forming SiO_2 in the direction normal to the Si surface, the free direction, which is given by the ratio σ_1 / η in the Maxwell model for a solid, also influences the oxidation rate at the interface. This form is arrived at because the stress relaxation process parallels the growth of oxide in the normal direction to the Si surface and relaxation away from the interface facilitates the formation of new oxide layers. The necessary volume for the new layers of oxide is created by the flow of the already formed SiO_2 away from the interface. The higher the stress and the lower the SiO_2 viscosity, the faster is the flow of formed oxide from the interfacial region and hence the more volume is available to the newly formed oxide. The above sited IR studies (28,29) also show that the bond angle profiles match the stress profiles at all temperatures studied, yielding sharper profiles for higher oxidation temperatures where relaxation takes place more readily. Thus the extent and the evolution with temperature of the stress profiles are corroborated by and consistent with several recent studies.

Sunmmary and Conclusions

The in-situ stress measurements performed in the present study confirm and extend the previous stress measurements on SiO_2 films on Si (8,11,22) as follows:

1. The existence and magnitude of an intrinsic compressive stress in SiO_2 formed vis thermal oxidation of Si is confirmed.

2. The magnitude of the thermal expansion stress is confirmed as are the literature values for the thermal expansion coefficients used for Si and SiO_2 as well as Youngs modulus for Si.

3. The profiles for σ_1 versus oxide thickness are confirmed in both magnitude and spatial extent.

4. The extent of the high stress region has been confirmed in independent SiO_2 film structural studies and is consistent with a previously proposed stress relaxation related oxidation model.

Acknowledgement

References

1. B.E. Deal and A.S. Grove, J. Appl. Phys., 36, 3770 (1965).

2. E.A. Irene and Y.J. van der Meulen, J. Electrochem. Soc., 123, 1380 (1976).

3. H.Z. Massoud, J.D. Plummer, and E.A. Irene, J. Electrochem. Soc., 132, 1745 (1985).

4. H.Z. Massoud, Ph.D. thesis, Stanford University, Stanford, CA, 1982.

5. E.P. EerNisse, Appl. Phys. Lett., 30, 290 (1977).

6. E.P. EerNisse, Appl. Phys. Lett., 35, 8 (1979).

7. E.A. Irene, E. Tierney, and J. Angillelo, J. Electrochem. Soc., 129, 2594 (1982).

8. E. Kobeda and E.A. Irene, J. Vac. Sci. Technol. B, 4, 720 (1986).

9. W.A. Tiller, J. Electrochem. Soc., 127, 625 (1980).

10. E.A. Irene, J. Appl. Phys., 54, 5416 (1983).

11. E. Kobeda and E.A. Irene, J. Vac. Sci. Technol. B, 5, 15 (1987).

12. E.A. Irene, H.Z. Massoud, and E. Tierney, J. Electrochem. Soc., 133, 1253 (1986).

13. R.H. Doremus, Thin Solid Films, 122, 191 (1984).

14. A. Fargeix and G. Ghibaudo, J. Appl. Phys., 56, 589 (1984).

15. G. Camera Roda, F. Santarelli, and G.C. Sarti, J. Electrochem. Soc., 132, 1909 (1985).

16. E.A. Irene and R. Ghez, Appl. Surf. Sci., 30, 1 (1987).

17. W. Kern and D.A. Poutinen, RCA Rev., 31, 187 (1970).

18. Corning Glass Works, Fused Silica, 7940 Data Sheets, Corning, New York, 1978.

19. L. Maissel, J. Appl. Phys., 44, 534 (1973).

20. G.G. Stoney, Proc. R. Soc. London Ser. A, **82**, 172 (1909).

21. W.A. Brantley, J. Appl. Phys., **44**, 534 (1973).

22. E. Kobeda and E.A. Irene, J. Vac. Sci. Technol. B, mar-apr 1988.

23. L.M. Landsberger and W.A. Tiller, Appl. Phys. Lett., **51**, 1416 (1987).

24. D.W. Hess and B.E. Deal, J. Electrochem. Soc., **124**, 735 (1977).

25. L.N. Lie, R.R. Razouk, and B.E. Deal, J. Electrochem. Soc., **129**, 2828 (1982).

26. T.Y. Tan and U. Goesele, Appl. Phys. Lett., **39**, 86 (1981).

27. G.M. Bartenev, <u>The Structure and Mechanical Properties of Inorganic Glasses</u> (Wolten-Noordhoff, Groningen, 1970).

28. J. Fitch, G. Lucovsky, E. Kobeda, and E.A. Irene, to be published.

29. G. Lucovsky, J. Fitch, E. Kobeda, and E.A. Irene, Proc. Electrochem. Soc. , May 1988.

Figure Captions

Figure 1. Schematic diagram of laser reflection technique
           modified to measure film stress at the oxidation
           temperature (not to scale).

Figure 2. Comparison of in-situ and room temperature film stress
           measurements as a function of oxide thickness.

Figure 3. Thermal stress vs. change in temperature, where the
           slope yields the product $E/(1-v)\Delta\alpha$.
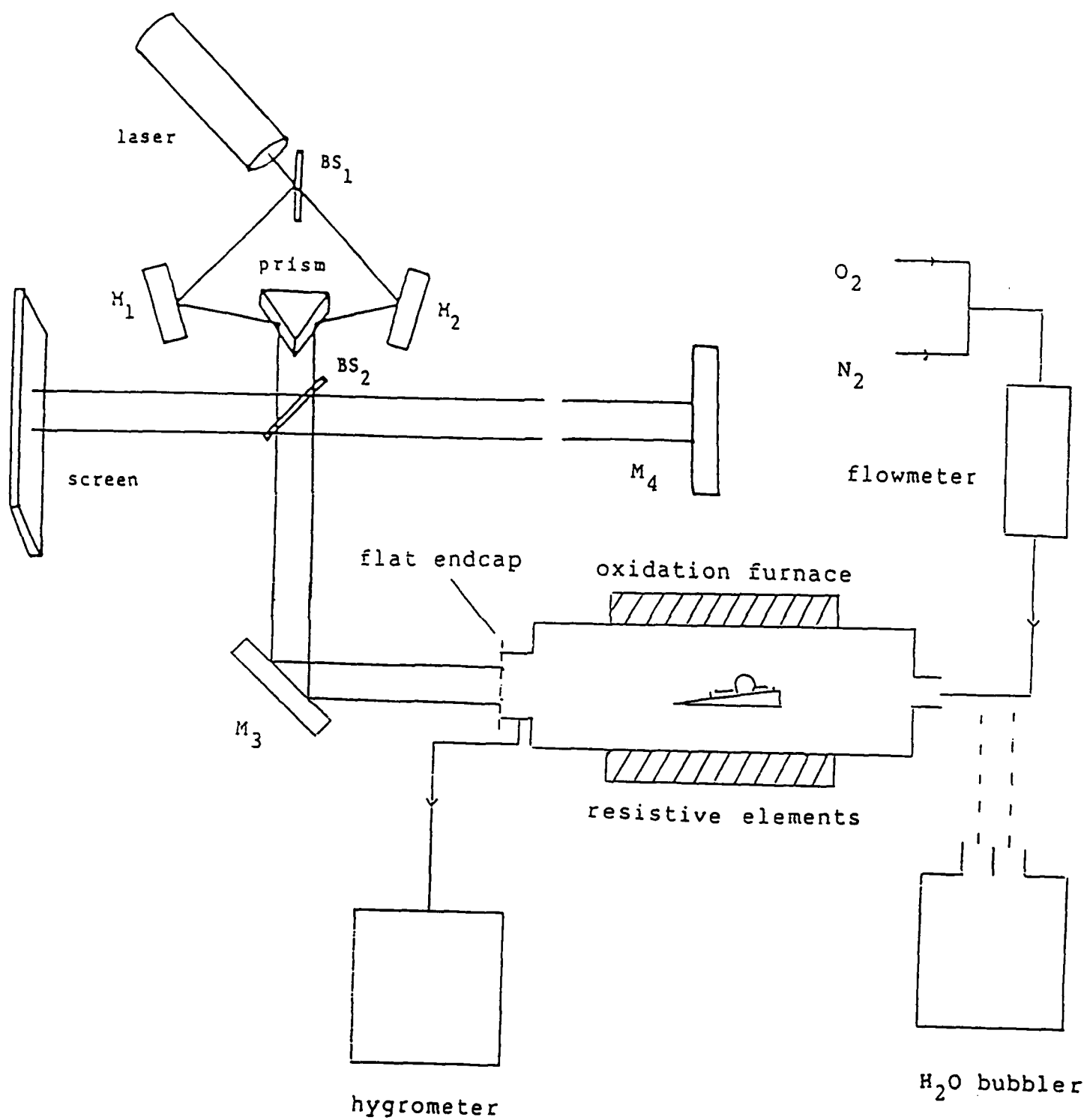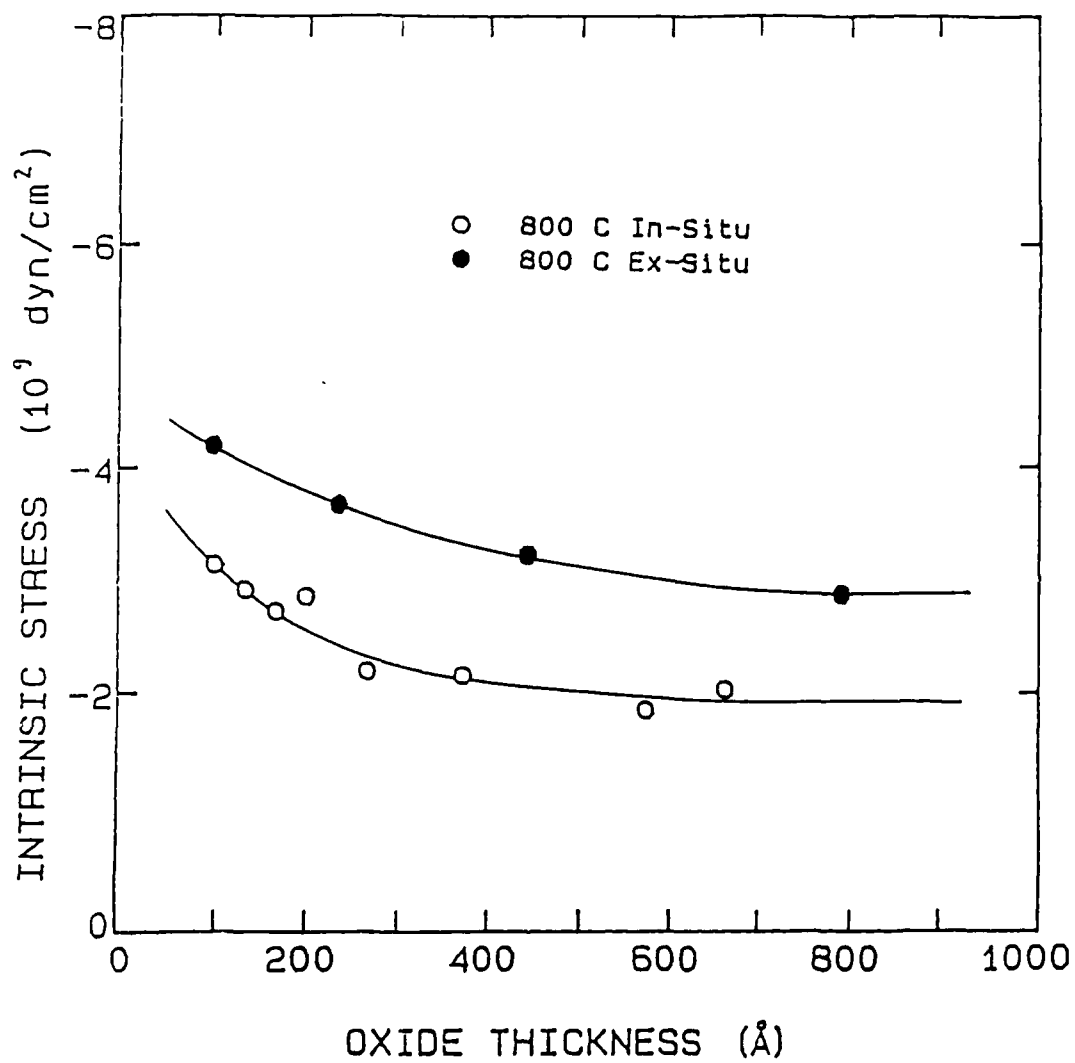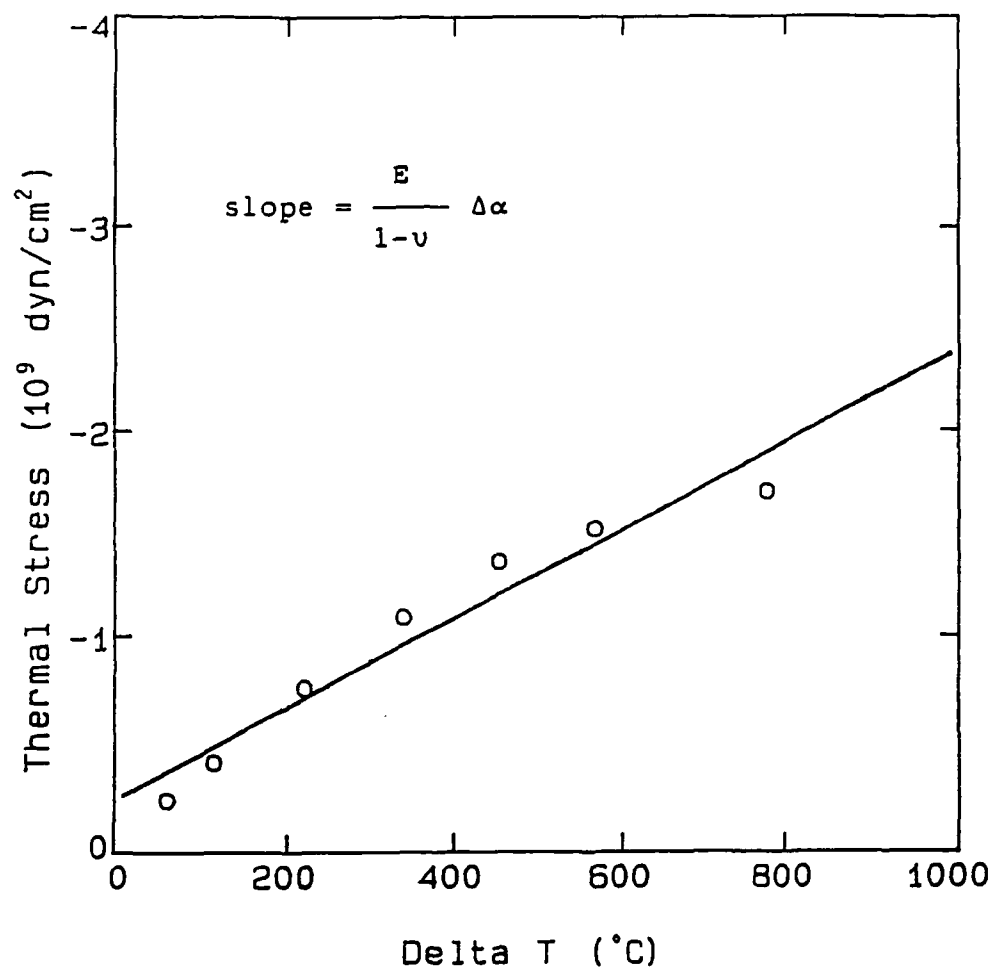
laser

BS₁

prism

M₁ M₂

BS₂

screen

M₄

flowmeter

O₂

N₂

flat endcap

oxidation furnace

M₃

resistive elements

hygrometer

H₂O bubbler

Fig 1

Fig 2

$$\text{slope} = \frac{E}{1-\nu} \Delta\alpha$$

Fig 3